Published as: *Neuron*. 2008 September 25; 59(6): 959–971.

A behavioral switch: cGMP and PKC signaling in olfactory neurons reverses odor preference in *C. elegans*

Makoto Tsunozaki[1,2], **Sreekanth H. Chalasani**[1], and **Cornelia I. Bargmann**[1]

1*Howard Hughes Medical Institute, Laboratory of Neural Circuits and Behavior, The Rockefeller University, New York, New York 10065*

2*Herbert W. Boyer Program in Biological Sciences, The University of California, San Francisco, California, 94143*

Summary

Innate chemosensory preferences are often encoded by sensory neurons that are specialized for attractive or avoidance behaviors. Here we show that one olfactory neuron in *Caenorhabditis elegans*, AWC^{ON}, has the potential to direct both attraction and repulsion. Attraction, the typical AWC^{ON} behavior, requires a receptor-like guanylate cyclase GCY-28 that acts in adults and localizes to AWC^{ON} axons. *gcy-28* mutants avoid AWC^{ON}–sensed odors; they have normal odor-evoked calcium responses in AWC^{ON}, but reversed turning biases in odor gradients. In addition to *gcy-28*, a diacylglycerol/protein kinase C pathway that regulates neurotransmission switches AWC^{ON} odor preferences. A behavioral switch in AWC^{ON} may be part of normal olfactory plasticity, as odor conditioning can induce odor avoidance in wild-type animals. Genetic interactions, acute rescue, and calcium imaging suggest that the behavioral reversal results from presynaptic changes in AWC^{ON}. These results suggest that alternative modes of neurotransmission can couple one sensory neuron to opposite behavioral outputs.

Introduction

Animals of many species are born with innate odor and taste preferences that cause them to approach food-related odors and avoid toxic substances. Experiments in nematodes, fruit flies, and mice have demonstrated that innate preferences are encoded, at least in part, by dedicated sensory neurons. In each animal, certain sensory neurons are preferentially coupled to attraction or food acceptance, while others drive aversion (Marella et al., 2006; Mueller et al., 2005; Tobin et al., 2002; Troemel et al., 1997; Zhao et al., 2003). Downstream of sensory neurons, the anatomical or physiological pathways for behavioral preference are largely undefined. At one extreme, there could be a complete labeled-line segregation of sensory projections, as proposed in *Drosophila*, where sweet and bitter taste fibers project to different target regions in the brain (Thorne et al., 2004; Wang et al., 2004). The flexibility of animal behavior, however, suggests that even innate sensory pathways may be sensitive to modification.

Chemosensory preference can be examined in detail in the nematode *C. elegans*, whose compact nervous system with 302 neurons allows functions to be mapped to specific cell types. *C. elegans* is attracted to chemicals sensed by two pairs of olfactory neurons called AWC and AWA and a pair of gustatory neurons called ASE (reviewed in Bargmann, 2006). It avoids

repulsive chemicals sensed by neurons called AWB, ASH and ADL. The sensory neurons detect environmental chemicals using G protein-coupled receptors (GPCRs) encoded by ~1700 chemoreceptor genes, as well as other receptors (Robertson and Thomas, 2006). Each sensory neuron expresses many chemoreceptor genes and detects many chemicals, an organization distinct from the one receptor-one neuron organization of the mammalian olfactory system. Sensory transduction downstream of *C. elegans* GPCRs is mediated either by cyclic guanosine monophosphate (cGMP) signaling through guanylate cyclases and cGMP-gated channels, or by signaling through transient receptor potential V (TRPV) channels, depending on the cell type (Bargmann, 2006).

In addition to the sensory properties defined by GPCRs, each sensory neuron is associated with a preferred behavioral output: attraction for AWC, AWA and ASE, and avoidance for AWB, ASH, and ADL. The strength of neuron-behavior coupling was demonstrated by expressing one receptor, the diacetyl-sensing GPCR ODR-10, in different sensory neurons (Troemel et al., 1997). Expression of ODR-10 in AWA or AWC neurons leads to attraction to diacetyl, whereas expression of ODR-10 in AWB leads to diacetyl avoidance (Sengupta et al., 1996; Troemel et al., 1997; Wes and Bargmann, 2001). The mechanisms by which AWA and AWC specify attraction and AWB specifies avoidance are not obvious, as these sensory neurons have largely overlapping synaptic targets (White et al., 1986).

Despite strong innate preferences, chemosensory behaviors of *C. elegans* can be altered by adaptation, sensitization, and associative learning. A striking change in behavior is caused by starving animals in the presence of NaCl, which is normally an attractive taste. Starvation/salt pairing for as little as ten minutes leads to salt avoidance, a reversal of normal behavior (Tomioka et al., 2006). In salt chemotaxis learning, an insulin signal from a downstream neuron activates an insulin receptor/PI 3-kinase signaling pathway within the ASER salt-sensing neuron to suppress its attractive activity (Tomioka et al., 2006). Mutation of the PI 3-kinase pathway eliminates salt chemotaxis learning, and constitutive activation by a mutation in the PTEN lipid phosphatase *daf-18* suppresses salt attraction. The ASER sensory neuron has a normal NaCl-evoked sensory response in calcium imaging of PI 3-kinase/*age-1* or PTEN/*daf-18* mutants, indicating that the PI 3-kinase pathway acts downstream of ASER sensory transduction, probably at the level of synaptic modulation (Tomioka et al., 2006). While ASER accounts for the loss of attraction after conditioning, the cellular mechanism of avoidance is less clear. One possibility is that ASER itself can direct attraction or repulsion depending on prior sensory experience (Tomioka et al., 2006). Alternatively, other sensory neurons may drive avoidance of NaCl when ASER's attractive role is silenced after conditioning. Several results support the second, multicellular model for avoidance. For example, if the ASH avoidance neurons are killed or inactivated, animals subjected to starvation/salt conditioning are no longer attracted to salt, but they do not avoid it (Hukema et al., 2006).

Here we examine a switch in olfactory preference in *C. elegans* and provide evidence that a single olfactory neuron can switch between attractive and avoidance behaviors, in violation of the pure labeled-line model. At a behavioral level, alternative chemosensory preferences are associated with reversed biases in turning frequency during odor chemotaxis. At a molecular level, two components of the behavioral switch are axonal cGMP signaling and a DAG/PKC signaling pathway that affects synaptic transmission. Specific sensory experiences alter the balance between attractive and repulsive behavioral states. These results suggest that axonal signaling pathways can rapidly respecify the connections between sensory neurons and behavioral outputs.

Results

gcy-28 mutations switch AWC^{ON} odor preference from attraction to avoidance

The two AWC sensory neurons sense partly overlapping groups of odors. The AWC^{ON} neuron senses butanone, the contralateral AWC^{OFF} neuron senses 2,3-pentanedione, and both AWC neurons sense benzaldehyde and isoamyl alcohol (Troemel et al., 1999; Wes and Bargmann, 2001). A screen for mutants defective in butanone chemotaxis yielded a notable mutant, *gcy-28 (ky713)*, that avoided butanone instead of approaching it (Fig. 1A, see Experimental Procedures). *gcy-28(ky713)* mutants avoided butanone across a range of concentrations that were attractive to wild-type animals (Fig. S1A). They showed reduced attraction, but not repulsion, to other odors sensed by AWC neurons, and were proficient in chemotaxis to odors sensed by AWA neurons (Fig. 1A). A deletion mutation in the *gcy-28* gene, *gcy-28(tm2411)*, had behavioral defects similar to those of *gcy-28(ky713)*.

The butanone avoidance defect in *gcy-28* mutants could be due to altered activity of AWC^{ON}, or due to altered function of other cells such as avoidance neurons. To distinguish between these possibilities, we examined mutants with defects in known cell types. *ceh-36* mutants lack AWC neurons due to a mutation in an Otx-type homeobox gene (Koga and Ohshima, 2004; Lanjuin et al., 2003). *gcy-28; ceh-36* mutants were not repelled by butanone, suggesting that AWC causes butanone avoidance in *gcy-28* mutants (Fig. 1B). Consistent with a defect in AWC, mutations in the AWC signal transduction genes *odr-1* and *tax-4*, which encode a ciliary guanylate cylase and a cyclic nucleotide-gated channel, respectively, also suppressed butanone avoidance of *gcy-28* mutants (Fig. S1B, data not shown). *gcy-28* butanone avoidance was not affected by a *lim-4* mutation that inactivates AWB avoidance neurons and ADF neurons, by an *osm-9* mutation that inactivates ASH and ADL avoidance neurons, or by a transgene that kills URX, AQR, and PQR oxygen-sensing neurons (Fig. S1C, S1D, and data not shown).

A marker for AWC^{ON}, *str-2*::GFP, was appropriately expressed in one AWC per animal in *gcy-28* mutants, suggesting that both AWC^{ON} and AWC^{OFF} were specified correctly (data not shown). To examine AWC^{ON} and AWC^{OFF} function independently, we used mutants that eliminated each cell type. *nsy-5* mutants have no AWC^{ON} cells but instead have two AWC^{OFF} cells (Fig. 1C) (Chuang et al., 2007), and *nsy-5 gcy-28* double mutants, like *nsy-5* mutants, were neither attracted to nor repelled by butanone (Fig. 1D). *nsy-1* mutants have two AWC^{ON} neurons and no AWC^{OFF} neurons (Fig. 1C) (Sagasti et al., 2001), and *gcy-28; nsy-1* double mutants showed enhanced avoidance of butanone compared to the *gcy-28* single mutants (Fig. 1E). These results suggest that AWC^{ON} is responsible for butanone avoidance in *gcy-28* mutants. To ask whether the *gcy-28* defect was butanone-specific or more general to AWC^{ON}, the double mutants were examined for benzaldehyde chemotaxis. *gcy-28; nsy-1* double mutants with two AWC^{ON} neurons avoided benzaldehyde (Fig. 1E). This result suggests that the AWC^{ON} neuron is systematically switched to an avoidance function in *gcy-28* mutants.

The AWC^{OFF} neuron is specifically required for chemotaxis to 2,3-pentanedione. *nsy-5*, *nsy-5 gcy-28* and *gcy-28; nsy-1* mutants all showed diminished attraction to 2,3-pentanedione, but not avoidance (Fig. 1D and E, Fig. S1E). Therefore, AWC^{OFF} function is reduced but not reversed by the *gcy-28* mutation. Reduced, but normal activity of AWC^{OFF} is also suggested by the partial recovery of benzaldehyde chemotaxis in *nsy-5 gcy-28* mutants with two AWC^{OFF} neurons (Fig. 1D), in contrast with the benzaldehyde avoidance of *gcy-28; nsy-1* mutants (Fig. 1E). Benzaldehyde chemotaxis in *gcy-28* single mutants was variable, as might be expected from an interaction of antagonistic signals from (repulsive) AWC^{ON} and (weakly attractive) AWC^{OFF} neurons.

As a further test of AWC^{ON} function in *gcy-28* mutants, we expressed the diacetyl receptor, ODR-10, in AWC^{ON} (Fig. 1F). In an *odr-10* mutant, expression of *odr-10* in AWC^{ON} restores attraction to diacetyl (Wes and Bargmann, 2001) (Fig. 1F). By contrast, in a *gcy-28;odr-10* double mutant, *odr-10* expression in AWC^{ON} causes animals to avoid diacetyl (Fig. 1F). Thus AWC^{ON} drives odor avoidance in *gcy-28* mutants.

gcy-28 mutants reverse the turning bias in AWC-mediated chemotaxis

To better understand both normal chemotaxis and the behavioral basis of the olfactory defects in *gcy-28* mutants, we analyzed olfactory chemotaxis using the framework of the biased random walk or "pirouette" model that was first developed for taste chemotaxis (Pierce-Shimomura et al., 1999). In the presence of attractive tastes, animals bias their turning frequency as a function of the concentration gradient, turning less when the concentration of an attractant is increasing and turning more when attractant concentration is decreasing (Pierce-Shimomura et al., 1999). This behavioral strategy results in eventual accumulation at an attractant source through a biased random walk, the mechanism of bacterial chemotaxis (Berg and Brown, 1972). Step changes in the concentration of the attractive odor isoamyl alcohol can regulate the turning rates of freely moving animals (Chalasani et al., 2007), or the turning of animals in liquid drops (Luo et al., 2008), but the turning response in odor gradients has not been examined.

Turning responses of *C. elegans* in odor gradients were observed by video microscopy of animals placed between a spot of odor and a spot of diluent (Fig. 2A and B). The frequency of turns was measured and classified as a function of the angle θ, where θ is the difference between the average direction of the animal's motion in a five-second window before the turn and the direction of the odor source (Fig. 2C). This angle approximates the concentration change the animal had been experiencing, with $\theta < 90°$ corresponding to increasing odor and $\theta > 90°$ corresponding to decreasing odor. Wild-type animals showed net movement toward the odor source (Fig. $2D_1$), increased their turning frequency when heading down the odor gradient, and reduced their turning frequency when heading up the gradient (Fig. $2D_2$, Fig. S2A). In the absence of odor, animals showed neither net migration nor turning bias (Fig. $2E_1$ and E_2). Wild-type animals had a similar turning bias in gradients of several attractive odors sensed by AWC neurons (Fig. 2G-I), and an opposite turning bias to the repulsive odor 2-nonanone, which is sensed by AWB neurons (Fig. S2C and D). These turning behaviors in odor gradients are consistent with a biased random walk model for positive and negative chemotaxis.

A similar analysis with *gcy-28* mutants revealed significant alterations of their turning bias. *gcy-28* mutants showed net movement away from a butanone source (Fig. $2F_1$), increased their turning frequency when heading up the odor gradient, and reduced their turning frequency when heading down the gradient (Fig. $2F_2$, Fig. S2B). In gradients of 2,3-pentanedione or benzaldehyde, *gcy-28* mutants showed little bias in turning frequency with respect to the odor gradient (Fig. 2H and I). Thus the regulated turning response of *gcy-28* mutants to different odors matched their accumulation in chemotaxis assays, with a reversed bias to butanone and no bias to benzaldehyde and 2,3-pentanedione.

To determine whether the turning bias was generated by AWC^{ON}, we used a laser microbeam to kill the AWC^{ON} neuron in wild-type animals and *gcy-28* mutants. Killing AWC^{ON} in wild-type animals abolished the net migration toward butanone (Fig. 3A)(Wes and Bargmann, 2001), and AWC^{ON}-ablated animals in a butanone gradient showed no turning bias going up or down the gradient (Fig. 3B). Killing AWC^{ON} in *gcy-28* animals abolished butanone avoidance (Fig. 3C) and eliminated the butanone-evoked turning bias (Fig. 3D). Overall rates of turning were unchanged after killing AWC^{ON}; only odor regulation was altered. These results indicate that AWC^{ON} is necessary for butanone avoidance in *gcy-28* mutants.

gcy-28 encodes a receptor-type guanylate cyclase

gcy-28(ky713) was mapped to the left arm of chromosome I using standard methods, and determined to affect the predicted gene T01A4.1 (*gcy-28*) (Fig 4A, Supplementary Material). *gcy-28* encodes several related receptor-type guanylate cyclases (rGCs), single-spanning transmembrane proteins with an extracellular ligand-binding domain and intracellular kinase-like and guanylate cyclase domains (Fig. 4B). Consistent with its sequence, the cyclase domain of *gcy-28* has guanylate cyclase activity when expressed in heterologous cells (Baude et al., 1997). Three splice forms of *gcy-28* were predicted from the genome sequence (T01A4.1a-c). We confirmed two of three forms by isolation of cDNAs (*gcy-28.a* and *gcy-28.c*, corresponding to T01A4.1a and T01A4.1c, respectively), and identified a fourth splice form, T01A4.1d (*gcy-28.d*), which fuses the upstream predicted gene T01A4.2 to T01A4.1 (Fig. 4A). The three confirmed *gcy-28* isoforms share predicted intracellular domains, but have alternative exons encoding the N-terminal extracellular domain. The *gcy-28(ky713)* mutation is a C to G transversion predicted to substitute a conserved phenylalanine for a leucine in the cyclase domain (Fig. 4C).

We subsequently obtained *gcy-28(tm2411)* (Shohei Mitani, National Bioresource Project, Japan), a deletion allele that results in a predicted frameshift upstream of the cyclase domain (Fig. 4A and B). The similar phenotypes of *gcy-28(ky713)* and *gcy-28(tm2411)* (Fig. 1A) suggest that strong loss-of-function mutations in *gcy-28* cause AWC chemotaxis defects.

The genome sequence of *C. elegans* predicts 27 genes for rGCs and seven soluble GCs (Morton, 2004; Ortiz et al., 2006). Many of the nematode cyclases result from unique expansions within the nematode clade, but some are shared by nematodes and other invertebrates (Fitzpatrick et al., 2006). *gcy-28* belongs to the natriuretic peptide receptor family of rGCs shared by both vertebrates and invertebrates (Fig. 4D). In mammals, natriuretic peptide signaling is important for proper regulation of blood pressure, cardiac myocyte growth, and bone development (Lopez et al., 1995; Oliver et al., 1997; Tamura et al., 2004; Tsuji and Kunieda, 2005). Although they are expressed in neurons in vertebrates, the role of natriuretic peptide receptors in the nervous system is largely unexplored.

GCY-28 can act in AWC to mediate chemotaxis

A reporter transgene driven by regions upstream of the *gcy-28.c* isoform has widespread expression in neurons and other tissues (Ortiz et al., 2006). We confirmed these results with additional reporters and found expression in almost all neurons, including AWC, as well as body wall muscle, gut, and hypodermis. The *gcy-28.a* upstream region was expressed in many, but not all, neurons, and the *gcy-28.d* upstream region was expressed in some neurons and in the gut.

A *gcy-28.c* cDNA expressed from its own promoter rescued the chemotaxis defects of *gcy-28* mutants, but failed to rescue when it included the *ky713* mutation (Fig. 5A). Heat-shock expression of *gcy-28.c* in adults resulted in behavioral rescue within two hours, indicating that the gene acts in mature neurons and not during nervous system development (Fig. 5B). The *gcy-28.c* isoform had high rescuing activity when expressed broadly (Fig. 5A-C) but incomplete rescuing activity when expressed only in AWC (Fig. 5D). By contrast, a *gcy-28.d* cDNA rescued chemotaxis when expressed under a pan-neuronal promoter (Fig. 5C), under the AWC-selective *odr-3* promoter (Fig. 5D), or under the AWC^{ON}-selective *str-2* promoter (Fig. 5E). The results with *gcy-28.c* suggest that *gcy-28* may have roles in multiple neurons; nevertheless, the full rescue with *gcy-28.d* suggests that *gcy-28* can function cell-autonomously in AWC^{ON}.

GFP-tagged isoforms of GCY-28.c and GCY-28.d had different subcellular localization in AWC. GCY-28.d, the more active isoform, was enriched in the axonal process, whereas GCY-28.c was present at equivalent levels in dendrites and axons (Fig. 5F). Both isoforms were present in the cell body and excluded from sensory cilia, in contrast with the cilia-localized rGCs ODR-1 and DAF-11, which function in sensory transduction (Birnby et al., 2000;L'Etoile and Bargmann, 2000). The axonal localization of GCY-28 suggests that it does not mediate primary sensory transduction in AWC.

To ask directly whether sensory transduction was affected in *gcy-28* mutants, we measured odor-evoked calcium transients in AWC^{ON} neurons expressing the genetically encoded calcium indicator G-CaMP. In both wild-type animals and *gcy-28* mutants, removing animals from butanone resulted in a strong increase in AWC^{ON} calcium levels, reported as an increase in G-CaMP fluorescence (Fig. 5G). These results are consistent with prior studies that suggest a hyperpolarizing, or inhibitory, mode of sensory transduction in AWC (Chalasani et al., 2007). Wild type and *gcy-28* showed similar AWC^{ON} responses across a range of butanone concentrations, and similar responses to other AWC-sensed odors (Fig. S3). In both wild-type and *gcy-28* mutant animals, calcium levels in AWC^{ON} were unchanged or decreased upon odor addition (Fig. 5G, Fig. S3). Thus *gcy-28* is not essential for the first steps of sensory transduction in AWC^{ON}.

gcy-28 interacts with axonal diacylglycerol and protein kinase C signaling

To establish a potential mechanism for cGMP effects on behavioral preference, we searched for mutations that resembled or suppressed *gcy-28*. A major effector of mammalian natriuretic peptide receptors is the cGMP-dependent kinase (PKG) (Potter et al., 2006). In *C. elegans* a PKG mutant, *egl-4*, has AWC chemotaxis and adaptation defects, as well as defects in other sensory behaviors (Daniels et al., 2000; Fujiwara et al., 2002; L'Etoile et al., 2002). However, close examination suggested that *egl-4* is not the primary target of cGMP from GCY-28: *egl-4* loss-of-function mutants had chemotaxis defects that were qualitatively different from *gcy-28* mutants, and the double mutant had defects different from either single mutant (Fig. S4A). Moreover, a gain-of-function mutation in *egl-4* did not suppress *gcy-28* butanone avoidance or other chemotaxis defects (Fig. S4B).

The presence of GCY-28 protein in axons suggested a possible role in regulation of synaptic function. To investigate this possibility, we examined mutations that alter synaptic transmission. *dgk-1* encodes a diacylglycerol (DAG) kinase that hydrolyzes DAG to phosphatidic acid (PA), and loss-of-function mutations in *dgk-1* increase DAG signaling and enhance cholinergic neurotransmission at the *C. elegans* neuromuscular junction (Lackner et al., 1999; Nurrish et al., 1999). A mutation in *dgk-1* strongly suppressed *gcy-28* chemotaxis defects (Fig. 6A), and this suppression was partially rescued by expressing a *dgk-1* cDNA in AWC (Fig. 6A). To ask whether this effect was due to increased DAG signaling or decreased PA signaling, we used a pharmacological agonist of DAG signaling, the synthetic β-phorbol ester phorbol 12-myristate 13-acetate (PMA) (Colon-Gonzalez and Kazanietz, 2006). Treating *gcy-28* mutants with PMA for two hours rescued their chemotaxis defects (Fig. 6B). Thus increased DAG signaling suppresses *gcy-28*, perhaps by affecting synaptic release.

One of the targets of DAG signaling is protein kinase C (PKC); previous work has shown that AWC chemotaxis requires the function of the *C. elegans* PKC *pkc-1/ttx-4* in AWC (Okochi et al., 2005). We found that the chemotaxis defect in *pkc-1* is similar to that of *gcy-28* (Fig. 6C): *pkc-1* mutants avoided butanone, while showing little preference for benzaldehyde. Functional Ca^{2+} imaging of AWC^{ON} cells in *pkc-1* mutants revealed normal butanone responses, suggesting that the *pkc-1* defect, like the *gcy-28* defect, is not in primary sensory transduction (Fig S5). *gcy-28; pkc-1* double mutants avoided butanone as much as *pkc-1* single mutants, suggesting that these two genes have related functions in AWC chemotaxis (Fig. 6C).

To further explore the similarity between *gcy-28* and *pkc-1*, we asked whether activation of PKC-1 in AWC might rescue *gcy-28* mutants. PKCs can be made constitutively active by an A160E mutation in the autoinhibitory pseudosubstrate motif (Dekker et al., 1993). Expression of PKC-1(A160E) in AWC fully rescued the chemotaxis defects of *gcy-28* mutants (Fig. 6D). Thus synaptic DAG signaling through PKC-1 may act downstream of or in parallel to GCY-28 to regulate the behavioral preference encoded by AWC^{ON}.

AWC sensory neurons synapse onto three classes of interneurons called AIB, AIY, and AIA (White et al., 1986). To ask whether the predicted change in AWC synaptic function might be observed in target neurons, we monitored butanone-evoked calcium responses in the AIB interneurons using G-CaMP. In wild-type animals, AWC has an excitatory connection with AIB, so AIB, like AWC, is activated by odor removal and inhibited by odor addition (Chalasani et al., 2007). AIB had a small but significant increase in calcium after butanone removal in wild-type animals, and a weaker but similar increase in *gcy-28* mutants (Fig. 6E). A difference between wild type and *gcy-28* was observed upon butanone addition: wild-type AIB neurons were inhibited by butanone, but *gcy-28* AIB neurons were not (Fig. 6E).

AWC olfactory preference changes with odor history

Certain odor conditioning protocols can lead to context-dependent, bidirectional modifications in AWC olfactory behavior. Odor conditioning in the absence of food causes adaptation, a reduction in chemotaxis (Colbert and Bargmann, 1995). Odor conditioning in the presence of food causes sensitization, or enhanced chemotaxis (Torayama et al., 2007). Previous studies have viewed these changes as increases or decreases in odor-specific AWC activity; we hypothesized that these context-dependent behaviors might, instead, affect the competing attractive and repulsive activities of AWC.

In the absence of food, conditioning wild-type animals with butanone for up to 90 minutes causes a butanone-specific reduction in chemotaxis (Colbert and Bargmann, 1995). We found that extending the conditioning to two hours led to butanone avoidance by wild-type animals (Fig. 7A). Long-term butanone conditioning also reduced benzaldehyde chemotaxis in wild-type animals, but did not affect chemotaxis to the AWC^{OFF} odor 2,3-pentanedione, suggesting a broader reduction of AWC^{ON} activity (Fig. 7A). The AWC^{ON} behaviors of butanone-adapted wild-type animals thus resembled the AWC^{ON} behaviors of naïve *gcy-28* mutants. In a *gcy-28* mutant, butanone adaptation did not cause stronger avoidance of butanone or reduced attraction to benzaldehyde, but instead reduced butanone avoidance (Fig. 7A; see also Fig. S7). These results suggest that *gcy-28* mutants occupy a behavioral state that wild-type animals enter after butanone adaptation.

Wild-type animals conditioned with butanone and food increase their chemotaxis to butanone (Fig. 7B). The sensitization response was intact in g*cy-28* mutants; in fact, conditioned *gcy-28* mutants were actually rescued, with levels of chemotaxis comparable to sensitized wild-type animals (Fig. 7B; see also Fig. S7). To determine if sensitization extended to all AWC^{ON} odors, animals were first conditioned with butanone and food, then tested for chemotaxis to benzaldehyde. Wild-type animals showed a small but consistent enhancement of benzaldehyde chemotaxis, and *gcy-28* animals showed striking rescue of their benzaldehyde chemotaxis defect (Fig. 7B). Butanone-induced sensitization did not affect 2,3-pentanedione chemotaxis (Fig. 7B). The pattern of odor responses suggests that butanone-induced sensitization caused a systematic enhancement of AWC^{ON}-mediated chemotaxis in both wild-type and *gcy-28* animals. The adaptation and sensitization experiments show that specific olfactory experiences can either mimic the *gcy-28* mutation, or rescue it.

Its widespread expression in the nervous system suggests that GCY-28 may have a role in other *C. elegans* behaviors. Indeed, *gcy-28* mutants had subtle defects in salt chemotaxis learning,

and they also had strong defects in the regulation of thermotaxis by starvation (Fig. S6) (Mohri et al., 2005;Tomioka et al., 2006). Although neither of these changes is as dramatic as the effect on AWC, they suggest that *gcy-28* signaling regulates multiple forms of sensory plasticity in *C. elegans*.

Discussion

A single-neuron switch between attraction and repulsion

Mutations in the receptor-type guanylate cyclase *gcy-28* lead to an avoidance behavior in place of the attractive behavior normally directed by the AWC^{ON} neuron. The behavioral defect in *gcy-28* mutants can be rapidly rescued by heat shock expression of *gcy-28*, by treatment with the DAG analog PMA, or, most strikingly, by conditioning animals briefly with butanone and food. These results suggest that AWC^{ON} neurons can switch rapidly between attractive and repulsive signaling modes.

A switch between attractive and repulsive signaling may contribute to wild-type behavior after odor adaptation or sensitization (Fig. 7C). The behavior of butanone-adapted animals resembles that of *gcy-28* mutants, and an analogy between the adapted state and the *gcy-28* mutant is suggested by the analysis of DAG signaling: genetic or pharmacological activation of DAG signaling in AWC neurons prevents adaptation in wild-type animals (Matsuki et al., 2006), and reverses the behavioral defects in *gcy-28* mutants. As a potential receptor, GCY-28 could transmit an internal signal about food or another cue to AWC. We suggest that the repulsive drive after adaptation is associated with low *gcy-28* activity and low DAG signaling, and the attractive drive from normal or sensitized AWC neurons is associated with high *gcy-28* activity, DAG signaling, and active *pkc-1*.

Many aspects of AWC^{ON} olfactory neurons revealed by this and other studies parallel those of the ASER gustatory neurons. Based on calcium imaging, both AWC^{ON} and ASER are OFF-sensing cells whose activity rises after decreases in attractive odors or tastes (Chalasani et al., 2007; Suzuki et al., 2008). In their normal attractive modes, both AWC^{ON} and ASER promote turning behavior when active. Finally, both AWC^{ON} and ASER are subject to plasticity that can reverse the polarity of sensory behavior (Hukema et al., 2006; Tomioka et al., 2006). In each case, the behavioral change is observed despite a normal or near-normal sensory OFF-response. Moreover, both switches involve molecules that regulate lipid signaling and possibly synaptic function -- *dgk-1* and *pkc-1* in AWC^{ON}, and $G_q\alpha$/*egl-30*, PI 3-kinase/*age-1*, and PTEN/*daf-18* in ASER (Tomioka et al., 2006).

For ASER, the behavioral switch after salt conditioning is regulated by a secreted insulin signal made by AIA interneurons (Tomioka et al., 2006). Several other neurons also contribute to salt plasticity, suggesting that conditioning affects multiple cell types. Although plasticity of the ASER neurons can fully explain the loss of attraction after conditioning, the switch to repulsion requires ASH avoidance neurons, ADF neurons, and URX, AQR, and PQR oxygen-avoidance neurons (Hukema et al., 2006). It is possible that ASER switches to an avoidance function, but it is not clear whether it does so. By contrast, our results show that repulsion directed by AWC^{ON} does not require any of the known avoidance neurons (AWB, ASH, ADL, URX, AQR, PQR) or ADF. Instead, AWC^{ON} appears to reverse its behavioral strategy directly, by changing its regulation of turning behavior during chemotaxis.

The gustatory ASE neurons and olfactory AWC neurons each have bilaterally asymmetric gene expression, and in each case the left-right pairs detect overlapping, but distinct, chemicals (Hobert et al., 2002). However, the functional asymmetry of these neurons is manifested differently in behavior. ASEL and ASER have reciprocal sensory and behavioral properties: unlike ASER, ASEL is an ON-sensing cell whose activity rises when attractive tastes appear,

and ASEL inhibits turning when active (Suzuki et al., 2008). AWC^{ON} and AWC^{OFF} are more similar; they are both OFF-sensing cells that stimulate turning when active (Chalasani et al., 2007). The AWCs differ, however, in their apparent sensitivity to the *gcy-28* and *pkc-1* signaling pathways, which reverse odor preference in AWC^{ON} but not in AWC^{OFF}. One interesting possibility suggested by the behavioral analysis of *gcy-28* turning behavior is that *gcy-28* switches AWC^{ON} between an ASER-like behavioral output that stimulates turning, and an ASEL-like behavioral output that inhibits turning.

Modulation of synaptic transmission may modify sensory preference

The similar chemotaxis phenotypes of *gcy-28* and *pkc-1* mutants and the genetic interactions between *gcy-28* and the DAG/PKC pathway suggest that these two signaling pathways regulate a common process in AWC^{ON}. The most likely possibilities are excitability or synaptic release. The most active GCY-28 isoform resides in axons, and while subject to the potential artifacts of GFP-tagged proteins, its localization suggests an interaction with the synaptic machinery. Synaptic transmission in vertebrate neurons can be regulated by cGMP-regulated protein kinases, cGMP-gated channels, and cGMP-regulated phosphodiesterases (Herring et al., 2001; Murphy and Isaacson, 2003; Richard and Bourque, 1996; Savchenko et al., 1997; Yu et al., 2006). DAG and phorbol esters modulate synaptic transmission by activating PKCs and Munc13/UNC-13 (Betz et al., 1998; Lackner et al., 1999; Shapira et al., 1987); in *C. elegans*, genetic or pharmacological manipulations that increase DAG enhance synaptic transmission, and PKC-1 regulates neuropeptide release (Nurrish et al., 1999; Lackner et al., 1999; Sieburth et al., 2007). The DAG/PKC synaptic signaling pathway is implicated in thermal behavioral plasticity, where DAG signaling affects the synaptic output of AFD thermosensory neurons (Okochi et al., 2005; Biron et al., 2006).

The altered butanone-evoked calcium signals in AIB are consistent with a change in synaptic function in *gcy-28* mutants. It is interesting that the defect appears mainly upon odor addition, which normally suppresses AIB activity, because it suggests that suppression and activation of AIB could each convey unique information. Electrophysiology in *Ascaris* has demonstrated that nematode motor neurons have graded neurotransmission; they release tonic transmitter at rest, increase release upon depolarization, and decrease it upon hyperpolarization (Davis and Stretton, 1989). If AWC^{ON} has similar synaptic properties, the altered AIB response in *gcy-28* could result from changes in tonic AWC^{ON} transmission, changes in hyperpolarization suppression of release, or an altered resting potential. These results should be interpreted with caution; the effects of *gcy-28* on AIB are subtle, and the cellular site of action has not been determined, so they could be direct or indirect.

There are several mechanisms by which *gcy-28* could alter turning behavior. AWC neurons use glutamate as a transmitter and also express neuropeptides, either of which could be regulated by *gcy-28* (Chalasani et al., 2007; Nathoo et al., 2001). *gcy-28* could redistribute the weights of AWC connections with its functionally distinct synaptic partners, AIA, AIB, and AIY (White et al., 1986; Chalasani et al., 2007). *gcy-28* could also alter the quality of AWC connection with individual synaptic partners: AWC normally activates the AIB target neuron and inhibits the AIY target neuron, but can activate AIY in certain receptor mutants (Chalasani et al., 2007). The biased random walk strategy for chemotaxis is intrinsically probabilistic and variable. Through relatively simple changes in synaptic weights or dynamics, the probabilistic circuit may have more flexibility to change its properties than deterministic circuits with fixed behavioral outputs.

GCY-28 is the sole *C. elegans* member of the natriuretic peptide receptor family, corresponding to vertebrate guanylate cyclase A (GC-A) and guanylate cyclase B (GC-B)(Potter et al., 2006). The natriuretic peptides do not have obvious homologs in the *C. elegans* genome; if there is a peptide ligand for GCY-28, it may have a distinct structure. Both GC-A and GC-B

are expressed in the vertebrate brain, and in the rat olfactory bulb (Gutkowska et al., 1997; Potter et al., 2006); it will be interesting to ask whether they have a role in olfactory behavior.

Context and experience modify sensory preferences in all animals. In *C. elegans*, we find that modulatory pathways acting in single sensory neurons can transform behaviors, allowing behavioral changes to emerge from changes in peripheral neurons. *C. elegans* has a small nervous system, but more complex animals also have anatomical pathways that support peripheral modulation. The mammalian olfactory bulb receives central innervation from adrenergic, serotonergic, and cholinergic fibers that could act as early as the presynaptic terminal of olfactory sensory neurons (Gomez et al., 2005). Our results suggest that modulatory information at this first synapse might generate qualitative differences in olfactory signaling, not just increases or decreases in sensory activity. Rapid behavioral switching provides a new view of the functional plasticity that can be generated within a fixed neuroanatomy.

Experimental Procedures

Standard techniques were used for nematode culture and molecular biology. A complete strain list, description of *gcy-28* cloning, detailed molecular biology, and sequence analysis methods are in Supplementary Material.

Behavioral assays

Population chemotaxis assays were performed on assay agar (1.6 % agar, 1 mM $MgSO_4$, 1 mM $MgCl_2$, 5 mM phosphate buffer, pH 6.0) in 10 cm square plates, which are better for detecting avoidance behavior than round assay plates (Troemel et al., 1997). Unless otherwise indicated, odor dilutions in ethanol were 2-butanone 1:1,000; 2,3-pentanedione 1:10,000; benzaldehyde 1:200; diacetyl 1:1,000; 2-methylpyrazine 1:1,000; 2-nonanone 1:10. 2 μl of diluted odor was placed on one side of the plate, and 2 μl of ethanol at the other side, with azide to anaesthetize animals that reached odor or ethanol sources. Washed adult animals were placed in the center of the plate, and the distribution of animals counted after 1-2 hours. A score of 1.0 represents perfect attraction, -1.0 perfect repulsion, and 0 random behavior. All data points are averages of ≥ 4 assays, with ≥ 50 animals each, repeated on at least two different days.

For tracking assays (Fig. 2, 3), about 50 animals were picked onto an NGM plate without bacteria, washed with S-basal and assay buffer, and placed on round 10 cm plates with assay agar. Excess liquid was wicked off, and recording was started after a spot of odor and diluent were placed on the agar surface. Unlike standard chemotaxis assays, no sodium azide was added. Tracking assays were performed under a dissecting scope (Stemi 2000; Zeiss, Thornwood, NY) with a custom-modified base that illuminates a wide field (Serco Technical Services, Livermore, CA). The field was captured by a digital camera (MacroFire; Optronics, Goleta, CA) with 1240×1240 pixel resolution at 2 frames per second. Captured movies were analyzed using MATLAB (MathWorks, Natick, MA) scripts (Ramot et al., 2008; http://wormsense.stanford.edu/). Tracks were segmented into turns and runs, essentially as described (Pierce-Shimomura et al., 1999). Runs were analyzed in 5-second bins, and an average bearing relative to the odor was obtained for each bin. Absolute angles were binned in 30° intervals.

PMA treatment was performed as described (Okochi et al., 2005). Briefly, adult animals were washed onto culture plates with 1 μg/ml PMA (PMA+) or DMSO solvent (PMA-) in the agar, incubated at room temperature for two hours, and then tested for chemotaxis in drug-free assay plates.

Heat shock treatment was performed as described (L'Etoile et al., 2002). Animals were incubated at 33°C for two hours, and then incubated for another two hours at 20°C before testing for chemotaxis.

Butanone sensitization assays were performed as described, with some modifications (Torayama et al., 2007). Animals on their NGM growth plate were exposed to butanone vapor by spotting 12 μL of butanone on agar plugs on the plate lid and sealing the plate with parafilm. After 90 minutes animals were washed and tested for chemotaxis on square plates. The butanone dilution used for chemotaxis was 1:1000. Adaptation assays were performed essentially as described (Colbert and Bargmann, 1995). Animals were washed and placed on 3% assay agar plates. 20 μL butanone was placed on agar plugs on the plate lid and the plates were sealed with parafilm. After two hours animals were washed off and tested for chemotaxis on square plates. Controls were treated identically except that butanone was omitted from the conditioning plate.

Laser ablations were performed on L1 animals as described (Bargmann and Avery, 1995). The AWC^{ON} cell was identified by expression of *str-2::GFP* in the integrated strain CX6343. About 20 animals were ablated for each tracking assay, and some animals were tested twice on two different days.

Calcium imaging

Calcium imaging was performed as described (Chalasani et al., 2007; Chronis et al., 2007). For AWC^{ON} imaging, the strain CX10281 expresses the calcium indicator G-CaMP2.0 (Tallini et al., 2006) in AWC^{ON} under the *str-2* promoter. *gcy-28(tm2411)* and *pkc-1(nj1)* were crossed into CX10281 to generate the strains CX10223 and CX10784, respectively. For AIB imaging, the strain CX7469 expressing G-CaMP1.0 in AIB neurons (Chalasani et al., 2007) was crossed with *gcy-28(tm2411)* to generate the strain CX8994. Animals were washed in buffer without food for ~20 minutes prior to imaging, a protocol designed to mimic the washes before chemotaxis assays. This brief washing step enhances the reliability of chemotaxis and of AWC calcium imaging. Imaging was conducted in a polydimethylsiloxane (PDMS) chamber in which an animal's nose was exposed to a stream of buffer that could be switched between odor-containing and odor-free solutions using an electronically gated valve. The standard stimulus protocol consisted of a 5-minute step pulse of the indicated dilution of odor in S-basal (without cholesterol) followed by odor removal. G-CaMP fluorescence intensity was measured for 10 seconds before and 50 seconds after the onset or offset of the odor stimulus; the same animals were imaged for odor onset and offset. All G-CaMP strains had the appropriate olfactory behaviors for their respective genetic backgrounds.

Supplementary Material

Refer to Web version on PubMed Central for supplementary material.

Acknowledgements

We thank the late David Garbers, Norio Suzuki, Isao Katsura, Loren Looger, the National Bioresource Project, and the *Caenorhabditis* Genetic Center (CGC) for strains and reagents; Daniel Ramot, Miriam Goodman, Jennifer Garrison, Navin Pokala, Carl Procko, and Shai Shaham for methods and advice; and members of the Bargmann lab for comments and discussions. MT designed and conducted genetic and behavioral experiments; MT and CHS conducted imaging experiments; MT and CIB interpreted results and wrote the paper. This work was funded by NIDCD and by the G. Harold and Leila Y. Mathers Charitable Foundation. CIB is an Investigator of the Howard Hughes Medical Institute.

References

Bargmann, CI. WormBook. Chemosensation in *C. elegans*. The *C elegans* Research Community, WormBook, 10.1895/wormbook.1.123.1. Oct 25. 2006 http://www.wormbook.org

Bargmann CI, Avery L. Laser killing of cells in *Caenorhabditis elegans*. Methods Cell Biol 1995;48:225–250. [PubMed: 8531727]

Baude EJ, Arora VK, Yu S, Garbers DL, Wedel BJ. The cloning of a *Caenorhabditis elegans* guanylyl cyclase and the construction of a ligand-sensitive mammalian/nematode chimeric receptor. J Biol Chem 1997;272:16035–16039. [PubMed: 9188508]

Berg HC, Brown DA. Chemotaxis in *Escherichia coli* analysed by three-dimensional tracking. Nature 1972;239:500–504. [PubMed: 4563019]

Betz A, Ashery U, Rickmann M, Augustin I, Neher E, Sudhof TC, Rettig J, Brose N. Munc13-1 is a presynaptic phorbol ester receptor that enhances neurotransmitter release. Neuron 1998;21:123–136. [PubMed: 9697857]

Biron D, Shibuya M, Gabel C, Wasserman SM, Clark DA, Brown A, Sengupta P, Samuel AD. A diacylglycerol kinase modulates long-term thermotactic behavioral plasticity in *C. elegans*. Nat Neurosci 2006;9:1499–1505. [PubMed: 17086178]

Birnby DA, Link EM, Vowels JJ, Tian H, Colacurcio PL, Thomas JH. A transmembrane guanylyl cyclase (DAF-11) and Hsp90 (DAF-21) regulate a common set of chemosensory behaviors in *Caenorhabditis elegans*. Genetics 2000;155:85–104. [PubMed: 10790386]

Chalasani SH, Chronis N, Tsunozaki M, Gray JM, Ramot D, Goodman MB, Bargmann CI. Dissecting a circuit for olfactory behaviour in *Caenorhabditis elegans*. Nature 2007;450:63–70. [PubMed: 17972877]

Chronis N, Zimmer M, Bargmann CI. Microfluidics for in vivo imaging of neuronal and behavioral activity in *Caenorhabditis elegans*. Nat Methods 2007;4:727–731. [PubMed: 17704783]

Chuang CF, Vanhoven MK, Fetter RD, Verselis VK, Bargmann CI. An innexin-dependent cell network establishes left-right neuronal asymmetry in *C. elegans*. Cell 2007;129:787–799. [PubMed: 17512411]

Colbert HA, Bargmann CI. Odorant-specific adaptation pathways generate olfactory plasticity in *C. elegans*. Neuron 1995;14:803–812. [PubMed: 7718242]

Colon-Gonzalez F, Kazanietz MG. C1 domains exposed: from diacylglycerol binding to protein-protein interactions. Biochim Biophys Acta 2006;1761:827–837. [PubMed: 16861033]

Daniels SA, Ailion M, Thomas JH, Sengupta P. *egl-4* acts through a transforming growth factor-beta/SMAD pathway in *Caenorhabditis elegans* to regulate multiple neuronal circuits in response to sensory cues. Genetics 2000;156:123–141. [PubMed: 10978280]

Davis RE, Stretton AO. Signaling properties of *Ascaris* motorneurons: graded active responses, graded synaptic transmission, and tonic transmitter release. J Neurosci 1989;9:415–425. [PubMed: 2563763]

Dekker LV, McIntyre P, Parker PJ. Mutagenesis of the regulatory domain of rat protein kinase C-eta. A molecular basis for restricted histone kinase activity. J Biol Chem 1993;268:19498–19504. [PubMed: 8396139]

Fitzpatrick DA, O'Halloran DM, Burnell AM. Multiple lineage specific expansions within the guanylyl cyclase gene family. BMC Evol Biol 2006;6:26. [PubMed: 16549024]

Fujiwara M, Sengupta P, McIntire SL. Regulation of body size and behavioral state of *C. elegans* by sensory perception and the EGL-4 cGMP-dependent protein kinase. Neuron 2002;36:1091–1102. [PubMed: 12495624]

Gomez C, Brinon JG, Barbado MV, Weruaga E, Valero J, Alonso JR. Heterogeneous targeting of centrifugal inputs to the glomerular layer of the main olfactory bulb. J Chem Neuroanat 2005;29:238–254. [PubMed: 15927786]

Gutkowska J, Antunes-Rodrigues J, McCann SM. Atrial natriuretic peptide in brain and pituitary gland. Physiol Rev 1997;77:465–515. [PubMed: 9114821]

Herring N, Zaman JA, Paterson DJ. Natriuretic peptides like NO facilitate cardiac vagal neurotransmission and bradycardia via a cGMP pathway. Am J Physiol Heart Circ Physiol 2001;281:H2318–2327. [PubMed: 11709398]

Hobert O, Johnston RJ Jr, Chang S. Left-right asymmetry in the nervous system: the *Caenorhabditis elegans* model. Nat Rev Neurosci 2002;3:629–640. [PubMed: 12154364]

Hukema RK, Rademakers S, Dekkers MPJ, Burghoorn J, Jansen G. Antagonistic sensory cues generate gustatory plasticity in *Caenorhabditis elegans*. EMBO J 2006;25:312–322. [PubMed: 16407969]

Koga M, Ohshima Y. The *C. elegans ceh-36* gene encodes a putative homemodomain transcription factor involved in chemosensory functions of ASE and AWC neurons. J Mol Biol 2004;336:579–587. [PubMed: 15095973]

L'Etoile ND, Bargmann CI. Olfaction and odor discrimination are mediated by the *C. elegans* guanylyl cyclase ODR-1. Neuron 2000;25:575–586. [PubMed: 10774726]

L'Etoile ND, Coburn CM, Eastham J, Kistler A, Gallegos G, Bargmann CI. The cyclic GMP-dependent protein kinase EGL-4 regulates olfactory adaptation in *C. elegans*. Neuron 2002;36:1079–1089. [PubMed: 12495623]

Lackner MR, Nurrish SJ, Kaplan JM. Facilitation of synaptic transmission by EGL-30 Gqalpha and EGL-8 PLCbeta: DAG binding to UNC-13 is required to stimulate acetylcholine release. Neuron 1999;24:335–346. [PubMed: 10571228]

Lanjuin A, VanHoven MK, Bargmann CI, Thompson JK, Sengupta P. Otx/otd homeobox genes specify distinct sensory neuron identities in *C. elegans*. Dev Cell 2003;5:621–633. [PubMed: 14536063]

Lopez MJ, Wong SK, Kishimoto I, Dubois S, Mach V, Friesen J, Garbers DL, Beuve A. Salt-resistant hypertension in mice lacking the guanylyl cyclase-A receptor for atrial natriuretic peptide. Nature 1995;378:65–68. [PubMed: 7477288]

Luo L, Gabel CV, Ha H, Zhang Y, Samuel AD. Olfactory behavior of swimming *C. elegans* analyzed by measuring motile responses to temporal variations of odorants. J Neurophysiol 2008;9:2617–2625. [PubMed: 18367700]

Marella S, Fischler W, Kong P, Asgarian S, Rueckert E, Scott K. Imaging taste responses in the fly brain reveals a functional map of taste category and behavior. Neuron 2006;49:285–295. [PubMed: 16423701]

Matsuki M, Kunitomo H, Iino Y. Goalpha regulates olfactory adaptation by antagonizing Gqalpha-DAG signaling in *Caenorhabditis elegans*. Proc Natl Acad Sci USA 2006;103:1112–1117. [PubMed: 16418272]

Mohri A, Kodama E, Kimura KD, Koike M, Mizuno T, Mori I. Genetic control of temperature preference in the nematode *Caenorhabditis elegans*. Genetics 2005;169:1437–1450. [PubMed: 15654086]

Morton DB. Invertebrates yield a plethora of atypical guanylyl cyclases. Mol Neurobiol 2004;29:97–116. [PubMed: 15126679]

Mueller KL, Hoon MA, Erlenbach I, Chandrashekar J, Zuker CS, Ryba NJ. The receptors and coding logic for bitter taste. Nature 2005;434:225–229. [PubMed: 15759003]

Murphy GJ, Isaacson JS. Presynaptic cyclic nucleotide-gated ion channels modulate neurotransmission in the mammalian olfactory bulb. Neuron 2003;37:639–647. [PubMed: 12597861]

Nathoo AN, Moeller RA, Westlund BA, Hart AC. Identification of neuropeptide-like protein gene families in *Caenorhabditis elegans* and other species. Proc Natl Acad Sci USA 2001;98:14000–14005. [PubMed: 11717458]

Nurrish S, Segalat L, Kaplan JM. Serotonin inhibition of synaptic transmission: Galpha(0) decreases the abundance of UNC-13 at release sites. Neuron 1999;24:231–242. [PubMed: 10677040]

Okochi Y, Kimura KD, Ohta A, Mori I. Diverse regulation of sensory signaling by *C. elegans* nPKC-epsilon/eta TTX-4. Embo J 2005;24:2127–2137. [PubMed: 15920475]

Oliver PM, Fox JE, Kim R, Rockman HA, Kim HS, Reddick RL, Pandey KN, Milgram SL, Smithies O, Maeda N. Hypertension, cardiac hypertrophy, and sudden death in mice lacking natriuretic peptide receptor A. Proc Natl Acad Sci USA 1997;94:14730–14735. [PubMed: 9405681]

Ortiz CO, Etchberger JF, Posy SL, Frokjaer-Jensen C, Lockery S, Honig B, Hobert O. Searching for neuronal left/right asymmetry: genomewide analysis of nematode receptor-type guanylyl cyclases. Genetics 2006;173:131–149. [PubMed: 16547101]

Pierce-Shimomura JT, Morse TM, Lockery SR. The fundamental role of pirouettes in *Caenorhabditis elegans* chemotaxis. J Neurosci 1999;19:9557–9569. [PubMed: 10531458]

Potter LR, Abbey-Hosch S, Dickey DM. Natriuretic peptides, their receptors, and cyclic guanosine monophosphate-dependent signaling functions. Endocr Rev 2006;27:47–72. [PubMed: 16291870]

Ramot D, Johnson BE, Berry TL Jr, Carnell L, Goodman MB. The Parallel Worm Tracker: a platform for measuring average speed and drug-induced paralysis in nematodes. PLoS ONE 2008;3:e2208. [PubMed: 18493300]

Richard D, Bourque CW. Atrial natriuretic peptide modulates synaptic transmission from osmoreceptor afferents to the supraoptic nucleus. J Neurosci 1996;16:7526–7532. [PubMed: 8922408]

Robertson, HM.; Thomas, JH. WormBook. The putative chemoreceptor families of *C. elegans*. The *C elegans* Research Community, WormBook, 10.1895/wormbook.1.66.1. Jan 06. 2006 http://www.wormbook.org

Sagasti A, Hisamoto N, Hyodo J, Tanaka-Hino M, Matsumoto K, Bargmann CI. The CaMKII UNC-43 activates the MAPKKK NSY-1 to execute a lateral signaling decision required for asymmetric olfactory neuron fates. Cell 2001;105:221–232. [PubMed: 11336672]

Savchenko A, Barnes S, Kramer RH. Cyclic-nucleotide-gated channels mediate synaptic feedback by nitric oxide. Nature 1997;390:694–698. [PubMed: 9414163]

Sengupta P, Chou JH, Bargmann CI. *odr-10* encodes a seven transmembrane domain olfactory receptor required for responses to the odorant diacetyl. Cell 1996;84:899–909. [PubMed: 8601313]

Shapira R, Silberberg SD, Ginsburg S, Rahamimoff R. Activation of protein kinase C augments evoked transmitter release. Nature 1987;325:58–60. [PubMed: 2432432]

Sieburth D, Madison JM, Kaplan JM. PKC-1 regulates secretion of neuropeptides. Nat Neurosci 2007;10:49–57. [PubMed: 17128266]

Suzuki H, Thiele TR, Faumont S, Ezcurra M, Lockery SR, Schafer WR. Functional asymmetry in *Caenorhabditis elegans* taste neurons and its computational role in chemotaxis. Nature 2008;454:114–117. [PubMed: 18596810]

Tallini YN, Ohkura M, Choi BR, Ji G, Imoto K, Doran R, Lee J, Plan P, Wilson J, Xin HB, et al. Imaging cellular signals in the heart in vivo: Cardiac expression of the high-signal Ca2+ indicator GCaMP2. Proc Natl Acad Sci USA 2006;103:4753–4758. [PubMed: 16537386]

Tamura N, Doolittle LK, Hammer RE, Shelton JM, Richardson JA, Garbers DL. Critical roles of the guanylyl cyclase B receptor in endochondral ossification and development of female reproductive organs. Proc Natl Acad Sci USA 2004;101:17300–17305. [PubMed: 15572448]

Thorne N, Chromey C, Bray S, Amrein H. Taste perception and coding in *Drosophila*. Curr Biol 2004;14:1065–1079. [PubMed: 15202999]

Tobin D, Madsen D, Kahn-Kirby A, Peckol E, Moulder G, Barstead R, Maricq A, Bargmann CI. Combinatorial expression of TRPV channel proteins defines their sensory functions and subcellular localization in *C. elegans* neurons. Neuron 2002;35:307–318. [PubMed: 12160748]

Tomioka M, Adachi T, Suzuki H, Kunitomo H, Schafer WR, Iino Y. The insulin/PI 3-kinase pathway regulates salt chemotaxis learning in *Caenorhabditis elegans*. Neuron 2006;51:613–625. [PubMed: 16950159]

Torayama I, Ishihara T, Katsura I. *Caenorhabditis elegans* integrates the signals of butanone and food to enhance chemotaxis to butanone. J Neurosci 2007;27:741–750. [PubMed: 17251413]

Troemel ER, Kimmel BE, Bargmann CI. Reprogramming chemotaxis responses: sensory neurons define olfactory preferences in *C. elegans*. Cell 1997;91:161–169. [PubMed: 9346234]

Troemel ER, Sagasti A, Bargmann CI. Lateral signaling mediated by axon contact and calcium entry regulates asymmetric odorant receptor expression in *C. elegans*. Cell 1999;99:387–398. [PubMed: 10571181]

Tsuji T, Kunieda T. A loss-of-function mutation in natriuretic peptide receptor 2 (Npr2) gene is responsible for disproportionate dwarfism in *cn/cn* mouse. J Biol Chem 2005;280:14288–14292. [PubMed: 15722353]

Wang Z, Singhvi A, Kong P, Scott K. Taste representations in the *Drosophila* brain. Cell 2004;117:981–991. [PubMed: 15210117]

Wes PD, Bargmann CI. *C. elegans* odour discrimination requires asymmetric diversity in olfactory neurons. Nature 2001;410:698–701. [PubMed: 11287957]

White JG, Southgate E, Thomson JN, Brenner S. The structure of the nervous system of the nematode *Caenorhabditis elegans*. Phil Trans R Soc Lond B 1986;314:1–340.

Yu YC, Cao LH, Yang XL. Modulation by brain natriuretic peptide of GABA receptors on rat retinal ON-type bipolar cells. J Neurosci 2006;26:696–707. [PubMed: 16407567]

Zhao GQ, Zhang Y, Hoon MA, Chandrashekar J, Erlenbach I, Ryba NJ, Zuker CS. The receptors for mammalian sweet and umami taste. Cell 2003;115:255–266. [PubMed: 14636554]

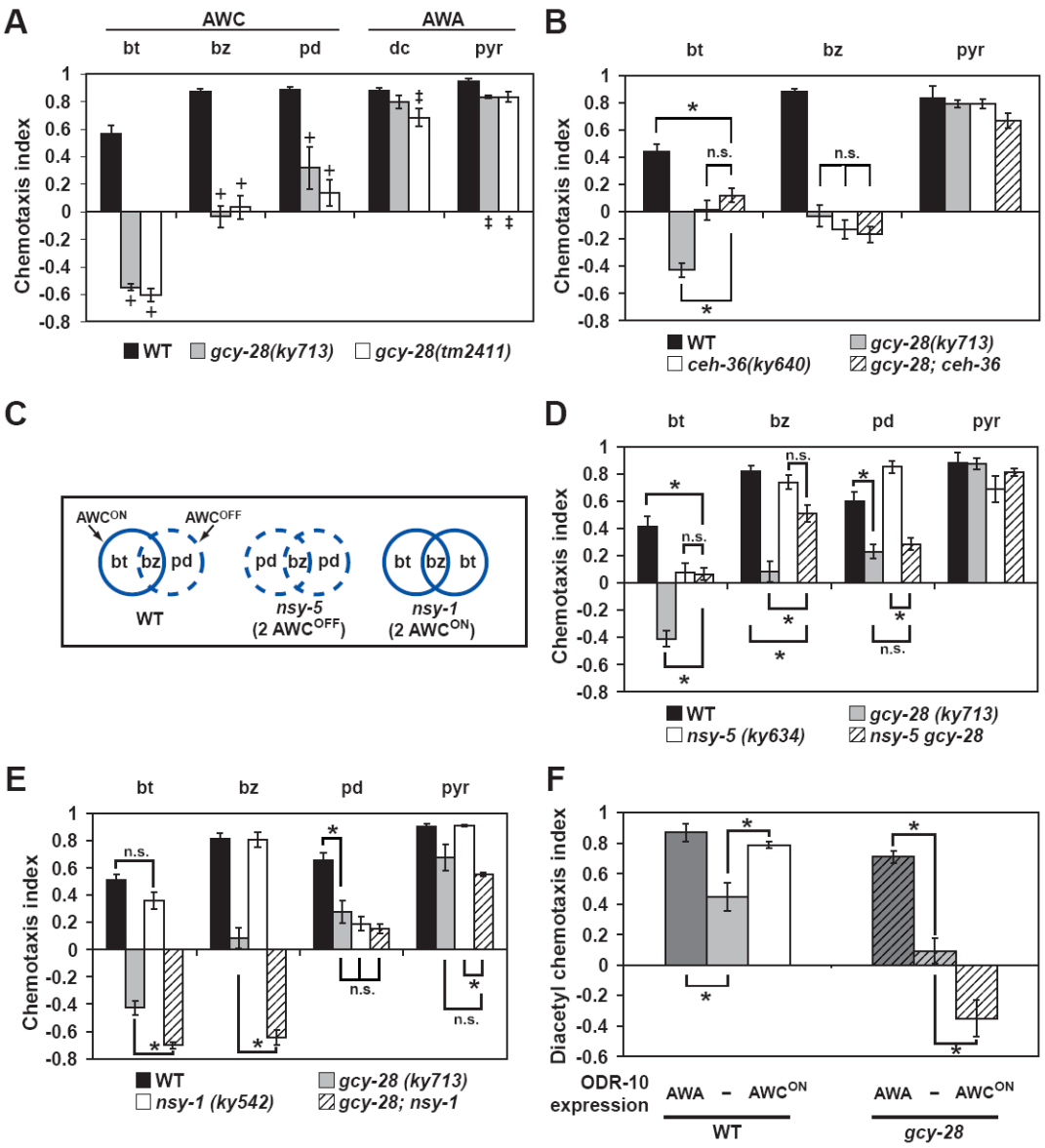

Figure 1. AWC^{ON} mediates odor avoidance instead of attraction in *gcy-28* mutants

(A) Chemotaxis of wild-type and *gcy-28* mutant animals to AWC- and AWA-sensed odors. (B) Effect of a *ceh-36* mutation on *gcy-28* chemotaxis. *ceh-36* mutants lack functional AWC and ASEL neurons. (C) Venn diagram representation of odor specificity in the AWC^{ON} (solid-line) and AWC^{OFF} (dashed-line) neurons. (D) Effect of a *nsy-5* mutation (2 AWC^{OFF} neurons) on *gcy-28* chemotaxis. (E) Effect of a *nsy-1* mutation (2 AWC^{ON} neurons) on *gcy-28* chemotaxis. (F) Diacetyl chemotaxis in strains misexpressing ODR-10 using the AWC^{ON}-selective *str-2* promoter. *odr-10* is normally expressed in AWA. + $p < 0.01$, ‡ $p < 0.05$ compared to wild type by Dunnett test. * $p < 0.05$, Bonferroni t-test. Error bars represent standard error of the mean (SEM). Abbreviations: WT, wild type; bt, 2-butanone; bz, benzaldehyde; pd, 2,3-pentanedione; dc, diacetyl; pyr, 2-methylpyrazine; n.s., not significant.

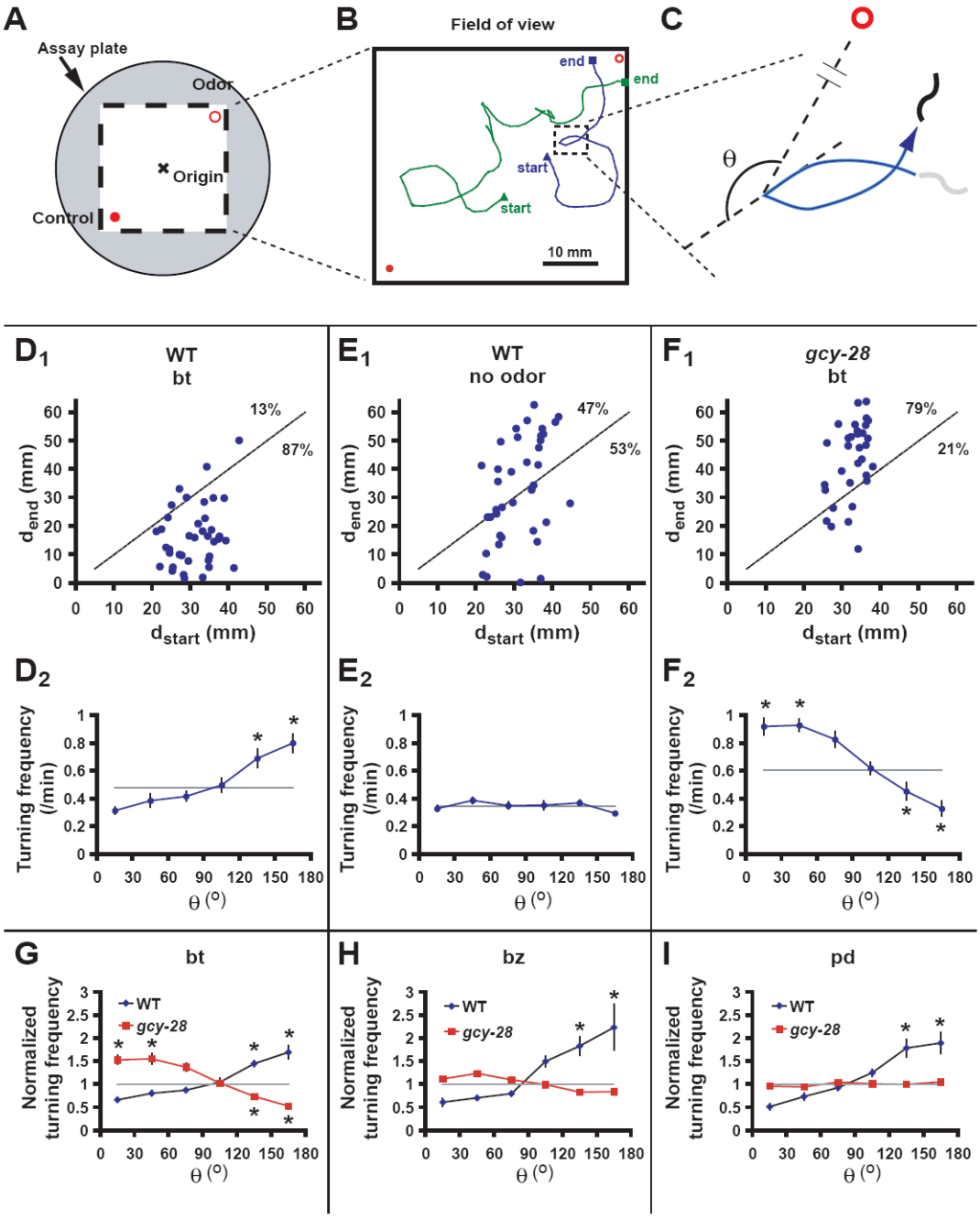

Figure 2. Regulated turning during chemotaxis to odors

(A) Chemotaxis tracking assay. The odor (open circle) and control (closed circle) spots were spaced 64 mm apart, and animals were placed at the origin. Behavior of animals was recorded for 15 minutes. (B) Representative tracks made by two wild-type animals migrating up a butanone gradient. The beginning and end of the tracks are marked. A track ends when the animal either exits the field of view or reaches within ~5 mm of the odor or the control spot. (C) A section of a track before and after a turning event. Angle θ represents the difference between the animal's direction of motion during a five-second interval before the turn and the direction to the odor. (D, E and F) Chemotaxis and regulated turning. (D_1, E_1, F_1) d_{start} and d_{end} represent the distance between the animal and the odor at the beginning and the end,

respectively, of an animal's track. Points below the diagonal are animals showing net migration toward the source; point above the diagonal, animals showing net migration away from the source. The percentages of animals above and below the diagonal are indicated. In the absence of odor (E), one control source was chosen arbitrarily as the reference point. Scatter plots are representative data from one assay each. (D_2, E_2 and F_2) Turning frequency plots representing averages of at least five assays each. The grey line represents the mean turning frequency over all assays for each condition. Wild-type animals showed no turning bias in the absence of odor (one-way ANOVA, $p > 0.1$). Similar turning biases were observed throughout the 15-minute assay (Fig. S2A and B). (G, H and I) Turning in gradients of different odors. Turning frequencies were normalized to the mean frequency of each individual assay. * $p < 0.05$ relative to the mean by Dunnett test. *gcy-28* animals showed no turning bias toward pd (one-way ANOVA, $p = 0.96$). *gcy-28* animals had a significant bias in response to bz by one-way ANOVA ($p = 0.003$) but a post-hoc Dunnett test showed no significant deviations from the average ($p > 0.05$). *gcy-28; nsy-1* double mutants, which avoid benzaldehyde (Fig. 1E), had a small but significant reversal in turning bias compared to wild-type (Fig. S2E and F). Error bars show SEM.

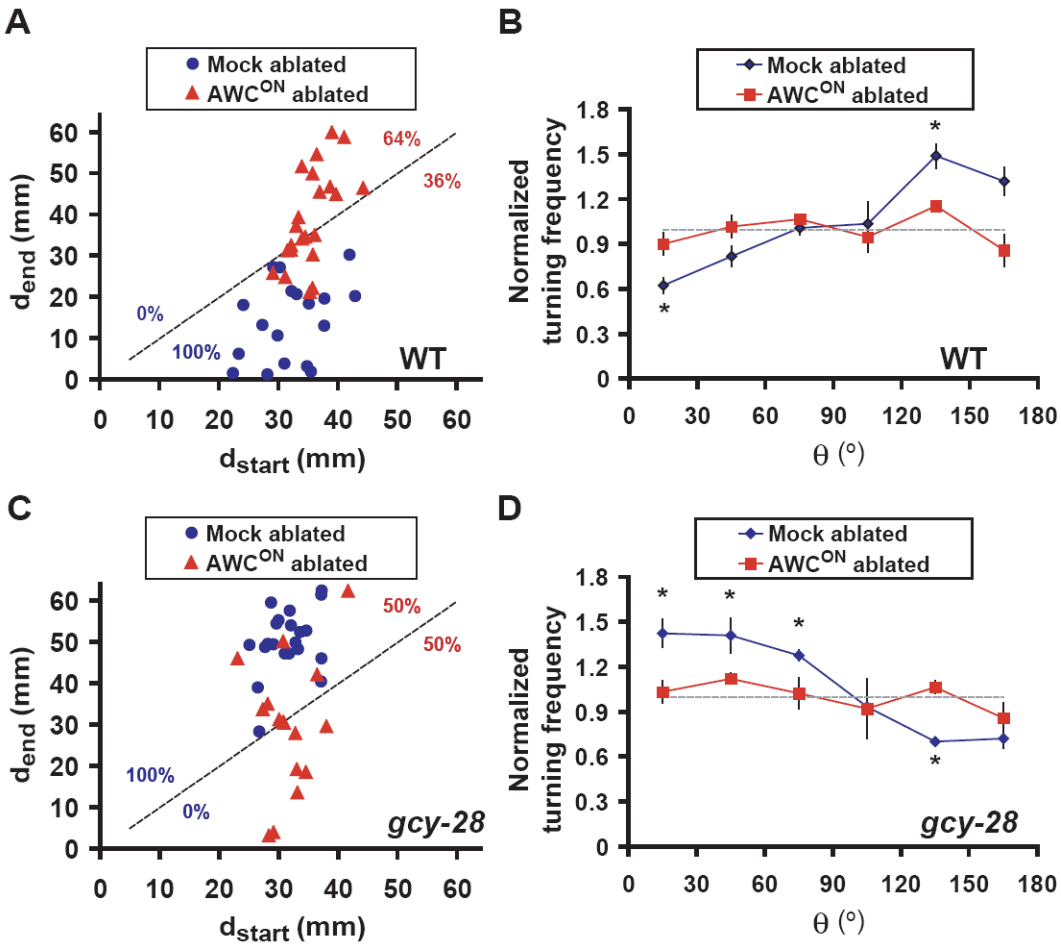

Figure 3. Ablation of AWC^{ON} abolishes turning bias in wild type and *gcy-28* animals

Tracking analysis of chemotaxis and turning bias in AWC^{ON}-ablated and control mock-ablated animals. (A and B) Wild-type animals. (C and D) *gcy-28(ky713)* mutants. In the scatter plots, the percentages of animals falling above or below the diagonal for mock- ablated and AWC^{ON}-ablated animals are indicated in blue and red, respectively. Net displacement ($d_{end} - d_{start}$) between mock and AWC^{ON}-ablated animals is significantly different for both wild-type and *gcy-28* animals (Mann-Whitney test, $p < 0.01$). Turning frequency is normalized to the mean frequency of each condition. Ablated animals do not show any significant turning bias (one-way ANOVA, WT: $p = 0.36$, *gcy-28*: $p = 0.85$). Turning frequencies are an average of three assays. Error bars represent SEM. * $p < 0.05$ relative to the mean by Dunnett test.

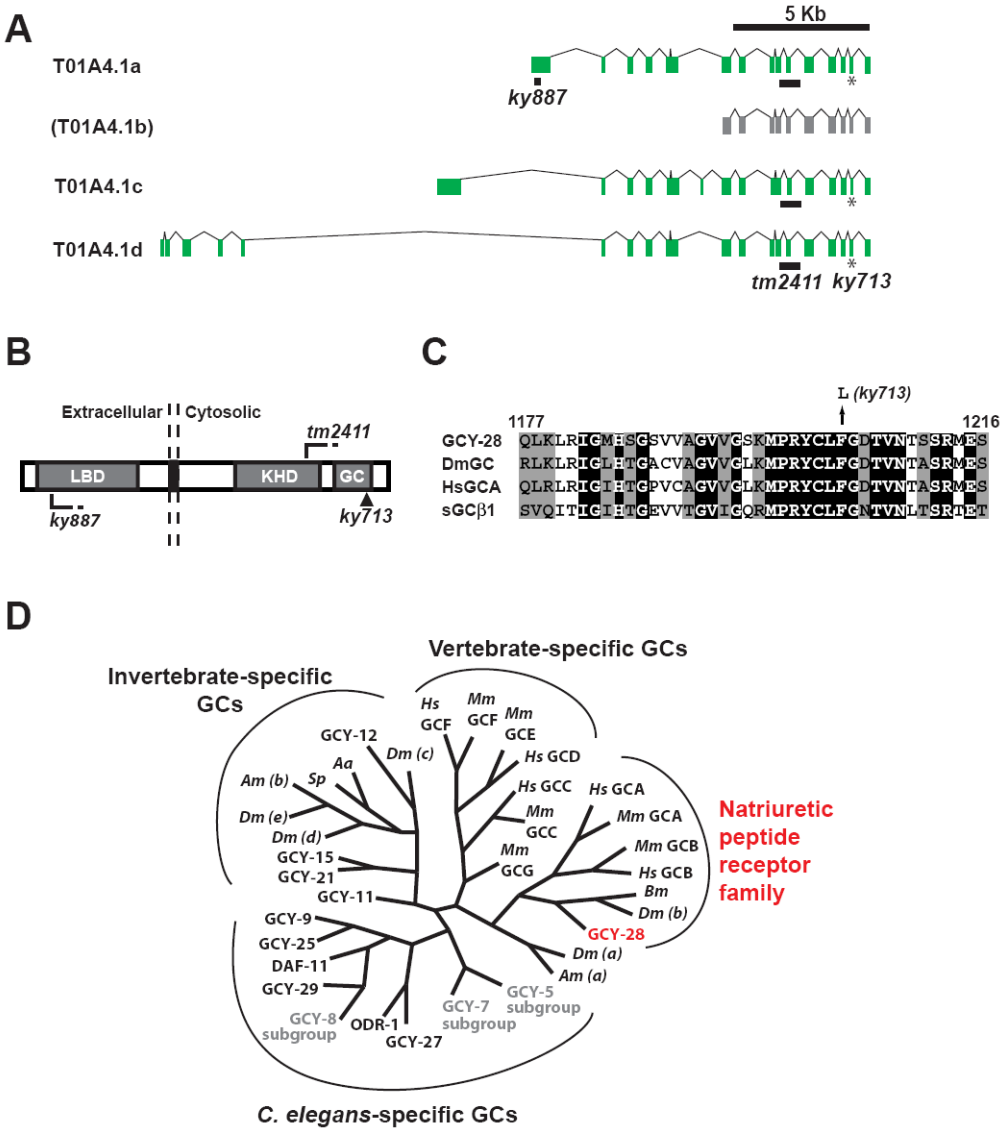

Figure 4. Sequence analysis of *gcy-28*

(A) Genomic organization of the *gcy-28* locus. Isoforms confirmed by cDNAs are shown in green. The first five exons of T01A4.1d were previously annotated in WormBase as a separate ORF, T01A4.2. Some T01A4.1c cDNAs lack the small exon 7 and some T01A4.1a cDNAs contain this exon. The *ky713* missense mutation is indicated by an asterisk, and two deletions (*tm2411* and *ky887*) are indicated by a line. *ky887* affects only T01A4.1a and has no chemotaxis defects (see Supplementary Methods). (B) Schematic of the domain structures of GCY-28 isoforms a, c and d. The approximate positions of the mutations are indicated. The alleles *tm2411* and *ky887* are deletions predicted to cause a frameshift. LBD – ligand-binding domain; KHD – kinase homology domain; GC – guanylate cyclase domain. (C) Alignment of part of the guanylate cyclase domains from different species. Conserved residues are shaded in black, similar residues are shaded in grey. The *ky713* mutation is F1204L. Numbers are relative to GCY-28.c. Abbreviations are: DmGC *Drosophila melanogaster* transmembrane guanylate cyclase; HsGCA *Homo sapiens* guanylate cyclase A; sGCβ1 *Homo sapiens* soluble guanylate cyclase β subunit. (D) Consensus tree of tmGCs. *C. elegans* tmGCs are GCYs, ODR-1 and DAF-11. The GCY-5 subgroup includes GCY-1, 2, 3, 4, 5, and 19; GCY-7 subgroup includes

GCY-6, 7, 14, 17, 20, and 22; GCY-8 subgroup includes GCY-8, 18, and 23 (Ortiz et al., 2006). Other species are abbreviated as follows: *Hs, Homo sapiens; Mm, Mus musculus; Dm, Drosophila melanogaster; Am, Apis mellifera; Bm, Bombyx mori; Aa, Asterias amurensis; Sp, Strongylocentrotus purpuratus*.

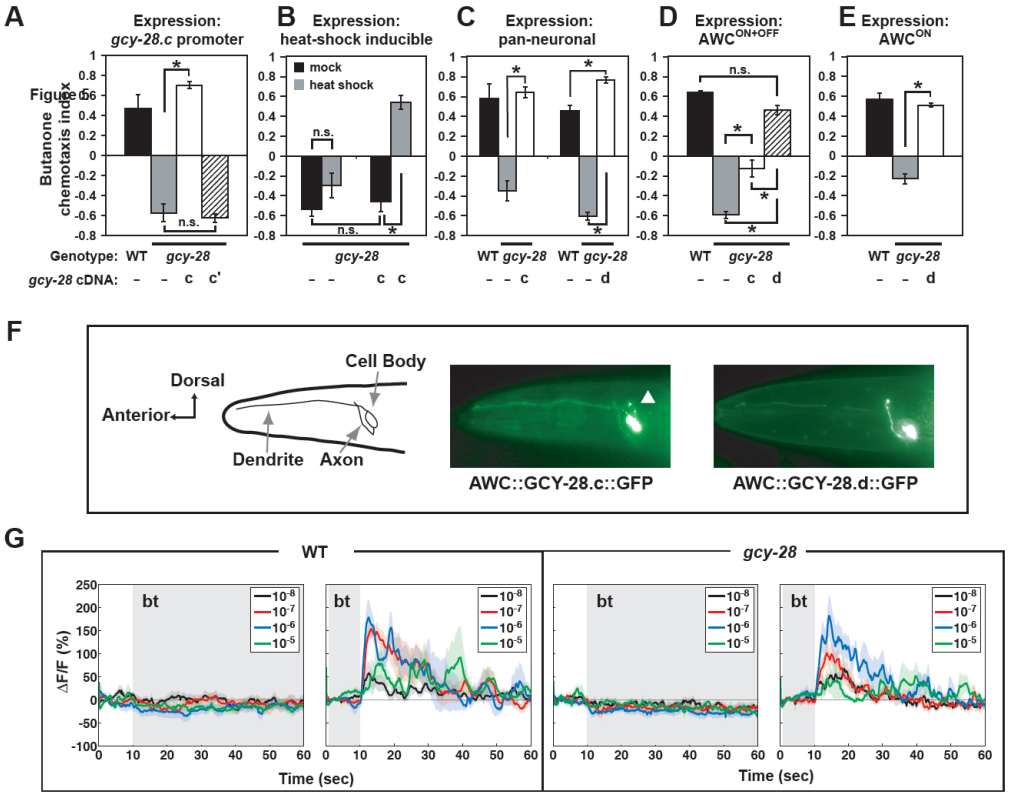

Figure 5. Spatial and temporal sites of GCY-28 action

(A-E) Butanone chemotaxis of *gcy-28(ky713)* mutants expressing different isoforms of *gcy-28* cDNAs under various promoters. Error bars represent SEM. * $p < 0.05$, Bonferroni t-test. (A) 3.2 Kb regulatory region upstream of *gcy-28.c* driving *gcy-28.c* cDNA. A cDNA with the *ky713* mutation is denoted c'. (B) Heat-shock inducible *hsp16-41* promoter driving *gcy-28.c* cDNA. (C) Pan-neural *H20* promoter driving *gcy-28.c* and *gcy-28.d* cDNAs. (D) AWC-selective *odr-3* promoter driving *gcy-28.c* and *gcy-28.d* cDNAs. (E) AWC^{ON}-selective *str-2* promoter driving *gcy-28.d* cDNA. (F) Subcellular localization of GFP-tagged GCY-28 expressed in AWC using the *odr-3* promoter. This promoter is expressed weakly in another olfactory neuron, AWB (arrowhead). (G) Average Ca^{2+} responses of AWC^{ON} neurons measured by changes in G-CaMP fluorescence in wild type and *gcy-28(tm2411)* animals. Grey shading indicates the presence of butanone. Legend indicates the dilution of butanone used as the stimulus. The left panels for each genotype show responses at the onset of the stimulus; the right panels show responses after removal of the stimulus. The shaded area around each trace represents the SEM. n = 7-11 animals for each condition.

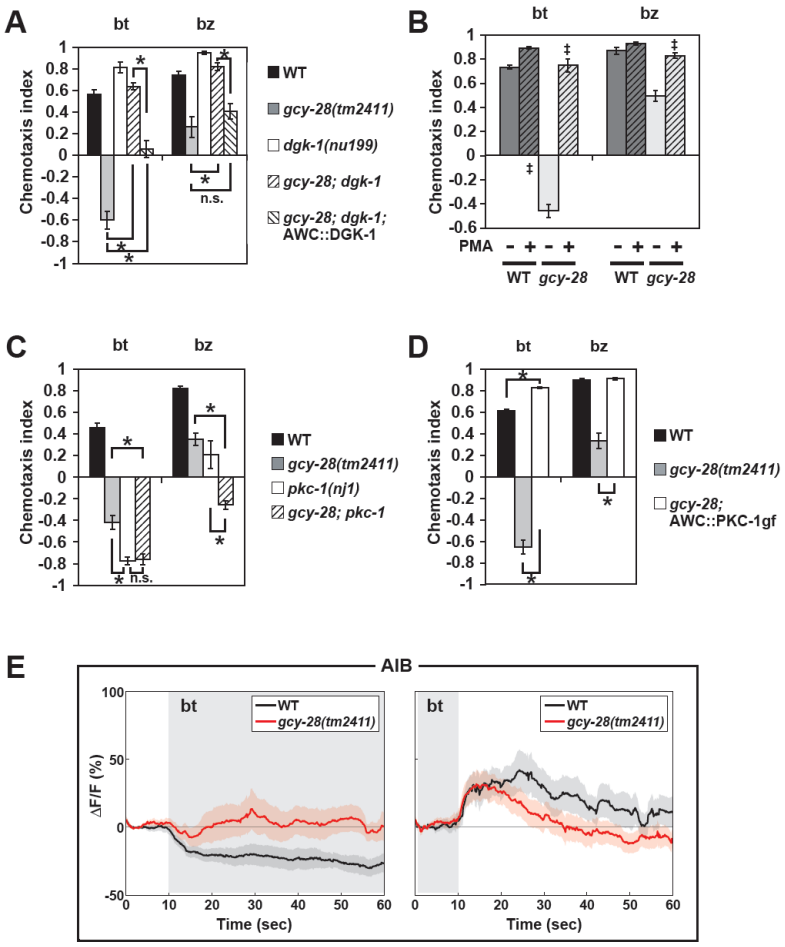

Figure 6. gcy-28 and DAG/PKC signaling interact to transform behavior

(A) Effect of a *dgk-1* mutation on chemotaxis of *gcy-28* mutants. For AWC-specific rescue of *dgk-1*, a *dgk-1.a* cDNA was expressed under the *odr-3* promoter. *dgk-1* single mutants carrying the rescuing array had chemotaxis indices comparable to wild-type animals (data not shown). (B) Chemotaxis of *gcy-28(tm2411)* mutants after treatment with 1 μg/ml PMA for 2 hours. (C) Chemotaxis of *pkc-1* and *gcy-28; pkc-1* double mutants. (D) Effect of expressing PKC-1 (A160E), a gain-of-function form of PKC-1, in AWC under the *odr-3* promoter. Expression in AWC^{ON} under the *str-2* promoter also rescued chemotaxis (data not shown). Error bars represent SEM. * $p < 0.05$, Bonferroni t-test, ‡ $p < 0.01$ relative to mock treated control, Student's t-test. (E) Average Ca^{2+} responses of AIB neurons measured by changes in G-CaMP fluorescence in wild type (n = 29) and *gcy-28(tm2411)* mutants (n = 27). Grey shading indicates the presence of butanone (10^{-6} dilution). Left panel, butanone onset; right panel, butanone offset after five minutes, in the same animals. The shaded area around each trace represents the SEM.

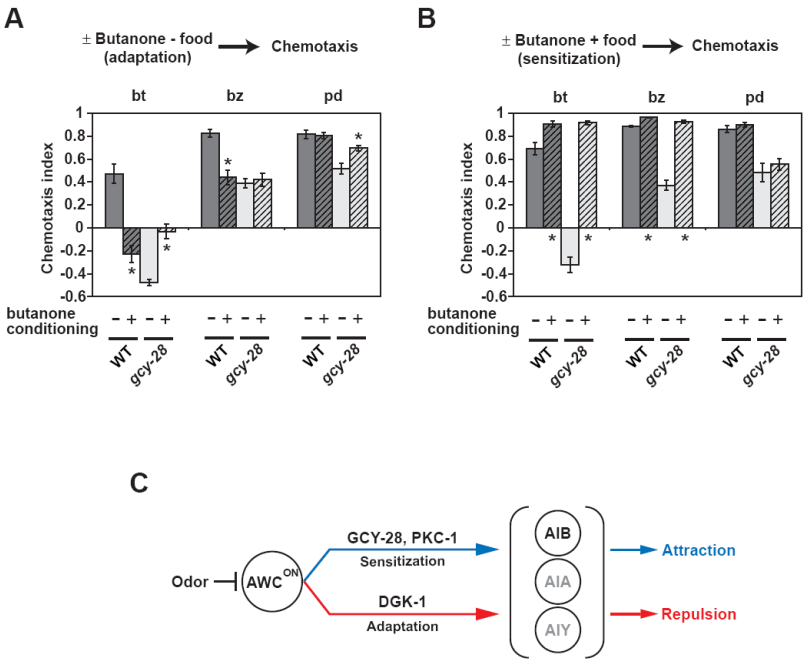

Figure 7. Olfactory plasticity is altered in *gcy-28* mutants

(A) Butanone adaptation in wild-type and *gcy-28(ky713)* mutant animals. Animals were incubated without food for 120 minutes, with or without butanone vapor (20 μL), then tested for chemotaxis to the indicated odors. Shorter adaptation protocols caused sensitization (rescue) of *gcy-28* mutants, consistent with a defect in starvation-odor integration (Fig. S7). (B) Butanone sensitization in wild-type and *gcy-28(tm2411)* mutant animals. Animals were incubated with food for 90 minutes, with or without butanone vapor (12 μL), then tested for chemotaxis to the indicated odors. Error bars represent SEM. * $p < 0.01$ relative to the respective control condition, Student's t-test. (C) Model for GCY-28 and DAG/PKC-1 signaling in AWC^{ON}. AWC^{ON} has two modes of synaptic communication with downstream interneurons (AIB, AIA, AIY), one driving attraction to odors and another driving avoidance of odors. GCY-28 and PKC-1 promote attraction in naïve animals, and DGK-1 promotes repulsion. Sensitization and adaptation favor attraction and repulsion, respectively.